RF-Magnetron Sputtering of Si_3N_4 and Study of Si_3N_4/*p*-Si Heterostructures

V. S. Zakhvalinskii[1,*], I. Yu. Goncharov[1], E. A. Kudryavtsev[1], E. A. Piluk[1], D. A. Kolesnikov[1], V. G. Rodriges[1], Z. A. Kabilov[1], S. V. Taran[1], and A. P. Kuzmenko[2]

[1] *Belgorod National Research University, Belgorod, 308015, Russia*
[2] *South-West State University, Kursk, 305040, Russia*

Here we report the feasibility of using cheap and environmentally friendly RF-magnetron sputtering of Si_3N_4 and formation of Si_3N_4 nanostructured films with developed surface. *p*-Si(100) polished plates commonly used in photovoltaic structures were chosen as a substrate. Si_3N_4 film surface morphology was studied using atomic force microscopy. It has been established that the specific surface area of the silicon nitride increases more than 10 times by increasing substrate temperature from $T_s = 40$ °C to $T_s = 800$ °C. At the same time, growth of substrate temperature changed the average size of nano-patterns. Cross section of the heterostructure Si_3N_4/*p*-Si(100) was investigated by high resolution transmission electron microscopy. Based on electron diffraction studies, it was found that the obtained silicon nitride film is a mixture of cubic and amorphous phases Si_3N_4. The Si_3N_4/*p*-Si(100) heterostructure is found to be similar to previously studied SiC/*p*-Si(100).

Keywords: RF Magnetron Sputtering, Si_3N_4 Thin Film, Nano-Patterns, Solar Cells.

1. INTRODUCTION

Silicon nitride (Si_3N_4) is one of the main dielectrics that are used in silicon electronics. As compared with silicon oxide ($\varepsilon \approx 3, 9$) nitride has a higher permittivity ($\varepsilon \approx 7$) and is used as an insulating layer. Besides, Si_3N_4 possesses the ability to localize (capture traps) injected into electrons and holes with a giant lifetime in a localized state, more than 10 years at 85 °C. Memory effect in silicon nitride is used in the non-volatile devices (flash memory).[1,2] For the silicon devices most commonly used amorphous silicon nitride. In photovoltaic structures amorphous silicon nitride is used as an anti-reflection layer with excellent surface and bulk passivation properties.[3]

Silicon nitride Si_3N_4 are yellowish crystals; polycrystalline Si_3N_4 color varies from white to gray. It is known in three modifications: α and β are of hexagonal syngony, for α-Si_3N_4 $a = 0.7765$ nm, $c = 0.5622$ nm, space group P31c; for β-Si_3N_4: $a = 0.7606$ nm, $c = 0.2909$ nm, space group P63/m; α-Si_3N_4 turns into β above 1400 °C, β-Si_3N_4 stable up to ~1600 °C. Cubic γ modification usually formed at high pressures, for γ-Si_3N_4 $a = 7.7418$ nm, space group Fd-3m. Si_3N_4 bandgap is 4.0 eV. Silicon nitride does not react with nitric acid, sulfuric acid and hydrochloric acid, slightly react with H_3PO_4 and intensively with hydrofluoric acid. Oxidation Si_3N_4 in air starts above 900 °C.[4] Unique chemical, mechanical, electrical and optical properties of silicon nitride make it promising material for electronics, including photovoltaics.

Layers of Si_3N_4 or related silicon nitride solid solutions are used in photovoltaic devices for the surface passivation[5] and as anti-reflective layers.[6] Electrical passivation is used to reduce the surface charge carriers' recombination in silicon wafers or films. Use of silicon nitride trap leads to a sharp reduction of carriers' concentration in the absorbing layer of the silicone wafer and decreases the probability of its recombination. As an antireflection layer Si_3N_4 increases light absorbtion.[3]

Particularly influential passivation effects should be pronounced on thin-film solar cells due to the fact that its surface is close to the space charge region of the *p*–*n* junction where charge separation occurs.[5]

In complex *p*–*i*–*n* solar cells there were used layers of amorphous Si_3N_4 or related silicon nitrides SiN_x and solid solutions based on Si_3N_{4-x}, which were deposited on the surface of the absorbing layer of Si emitter. In some cases, passivation layers were deposited before applying a back electrode.[3,8] There are approved performance improvement of industrial photovoltaic cells after Si_3N_4 application passivation layers of hydrogenated amorphous silicon nitride

a-SiN$_x$:H using plasma-enhanced chemical vapor deposition (PECVD). In many cases the addition of small amounts of hydrogen, that is often used in the passivation layers in solar cells did not significantly affect the crystal structure and electronic properties of silicon nitride.[9]

For preparation of amorphous hydrogenised films there are known varieties of chemical vapor deposition technology (CVD): hot wire CVD (HWCVD), hot filament CVD (HFCVD) or catalytic CVD (Cat-CVD).[10–12] CVD technologies are environmentally harmful because of the toxic chemicals used. Environmentally friendly alternatives are high frequency magnetron sputtering (RF-magnetron sputtering) or laser ablation (LA).

Moreover, in order to reduce the cost of solar panels it is reasonable to use the simplest single-junction structures.[7] Efficiency of solar cells could be improved by increased absorption of the upper layer of the heterostructure provided by Si_3N_4 films. The high frequency magnetron sputtering allows obtaining a homogeneous, developed surface of the absorbing layer. Regime of sputtering can control surface morphology and device structure.

In this work we report the obtaining of Si_3N_4/Si(100) layer with a developed surface and its properties as a function of preparation procedure.

2. EXPERIMENTAL DETAILS

2.1. Preparation of Si_3N_4 Nanolayers

Thin films of partially amorphous nanocrystalline Si_3N_4 were prepared by the high-frequency non-reactive magnetron sputtering in an Ar atmosphere using an improved Ukrrospribor VN-2000 setup. A previously synthesized silicon nitride was used as a target. Deposition was carried out on a polished (100) plane of p-Si with a resistivity of 2 Ohm · cm. Optical heating allowed to control the substrate temperature in the range from 40 to 800 °C. It has been found that on unintentional substrate heating

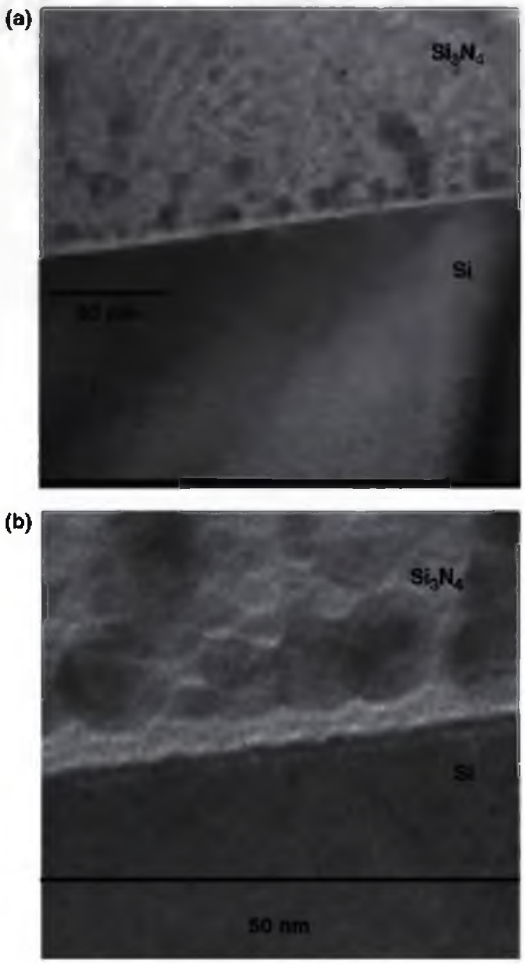

Fig. 1. Findings of investigation of thin foil cross section of heterostructure Si_3N_4/Si(100) in transmission electron microscope (TEM). (a) Interface overall view of heterostructure Si_3N_4/Si(100). (b) Composite morphology of Si_3N_4 film cross section.

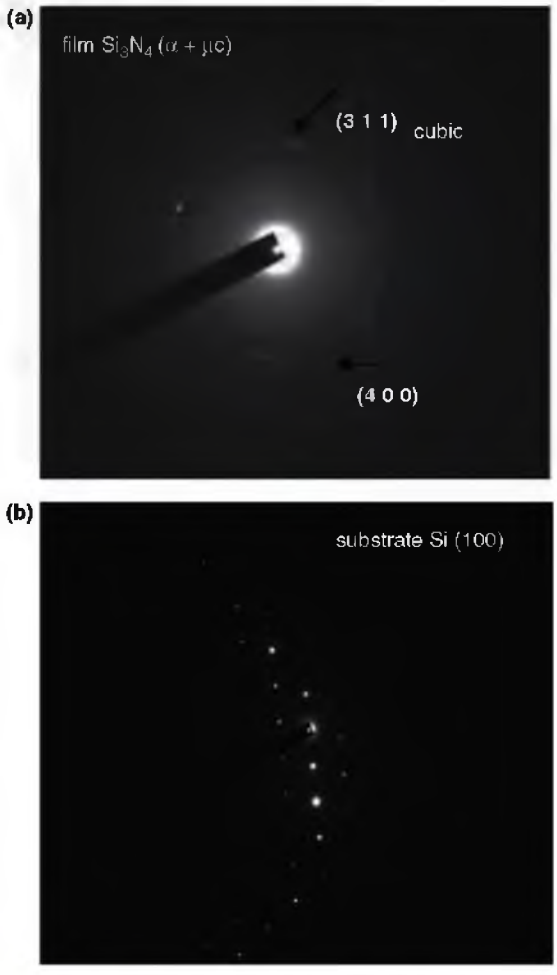

Fig. 2. Electron diffraction from Si_3N_4/Si(100) heterostructure obtained in transmission electron microscope (TEM). (a) Diffusional rings around reflection diffusional center indicate dominant amorphous nature of the film, availability of ill-defined concentric rings indicates minor phase of nanocrystallic or fine-grained nature. (b) For comparison there is shown electron diffraction image obtained for Si(100) monocrystallic substrate in the same heterostructure.

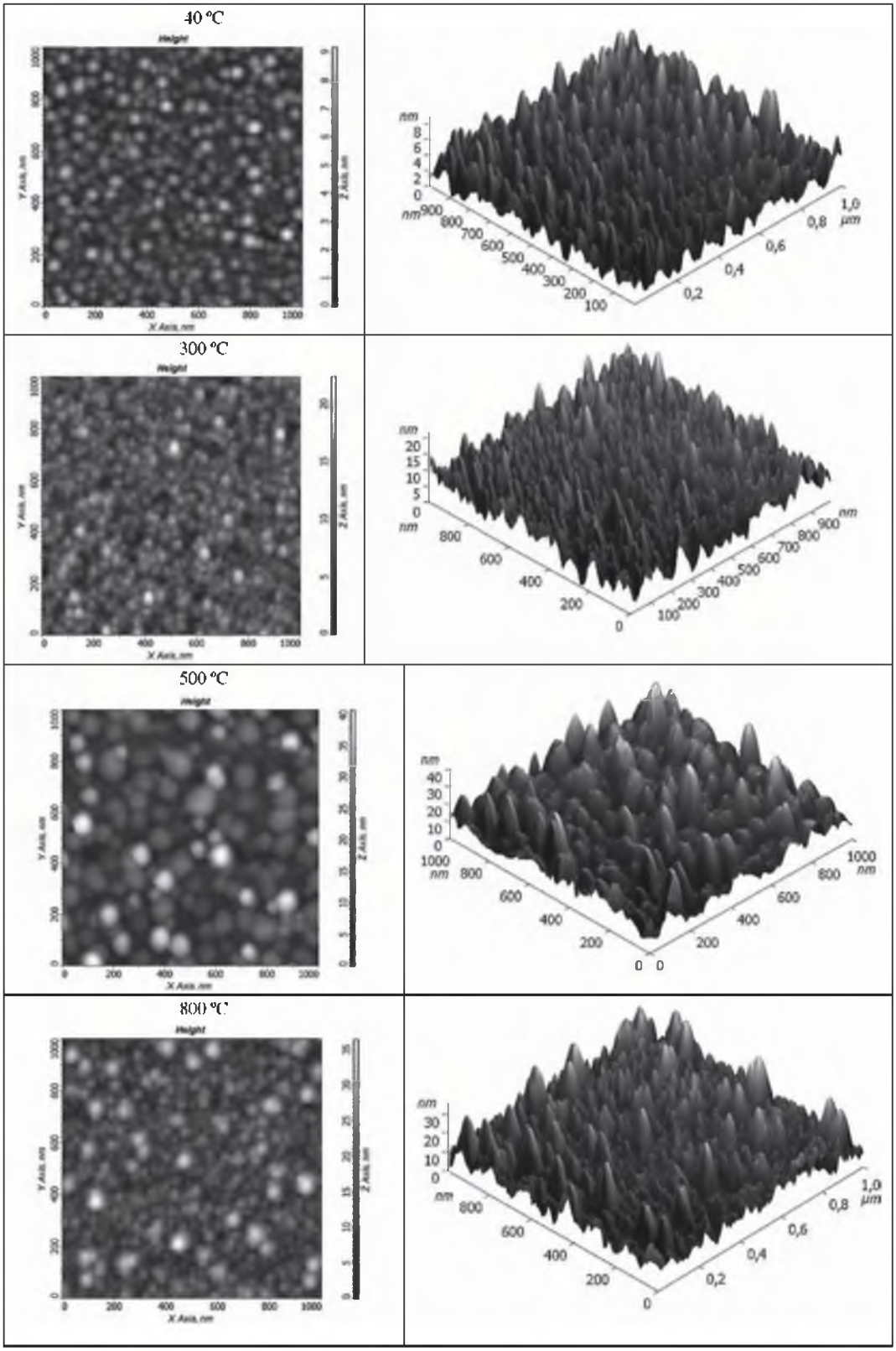

Fig. 3. AFM results for Si_3N_4 film surfaces obtained during high frequency magnetron deposition with temperatures of Si(100) substrate of $T_S = 40$, 300, 500 и 800 °C, respectively.

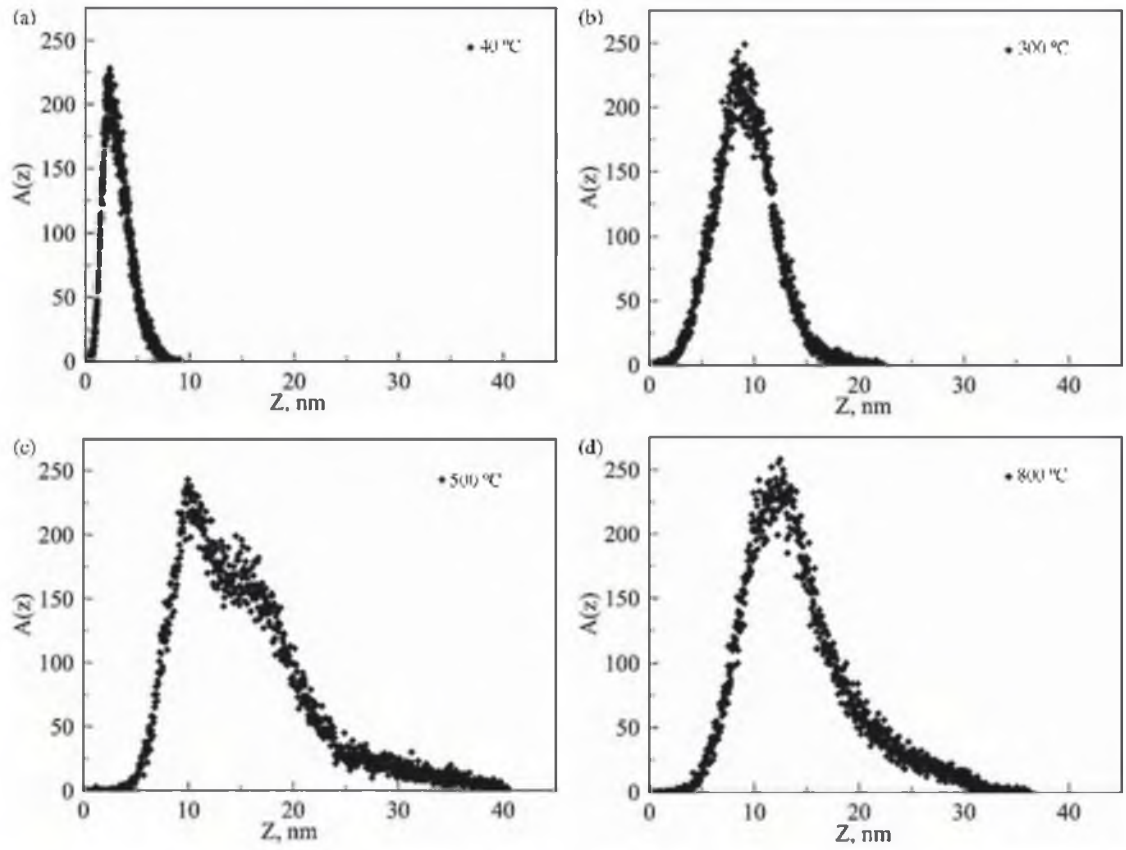

Fig. 4. Evolution of altitude assignment function A(Z) of thin films Si_3N_4 obtained for temperatures Si substrate $T_s = 40$ °C, 300 °C, 500 °C and 800 °C.

its temperature was about 40 °C due to interaction with the plasma. The layer of silicon oxide was removed from Si substrate by chemical etching in HF before the Si_3N_4 film deposition. Si_3N_4 nanolayers with the thickness of about 20 nm have been deposited at 40, 300, 500 and 800 °C.

2.2. Characterization of Si_3N_4 Nanolayers and Si_3N_4/Si(100) Heterostructure

The vibration structure of deposited layers was characterized by Raman spectroscopy using co-focal nanometric resolution Omega Scope AIST-NT Raman microscope excited with an 532 nm Ar^+ laser. The Raman spectra

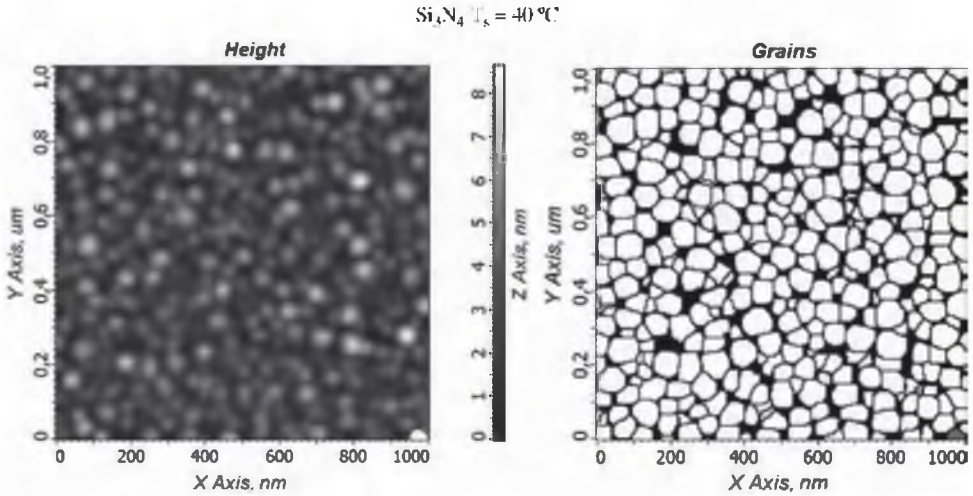

Fig. 5. On the left part of the figure it is shown the AFM image of a Si_3N_4 film obtained during high-frequency magnetron deposition on the surface under temperature $T_s = 40$ °C. On the right part of figure it is shown the image of surface, ready for statistical treatment procedure.

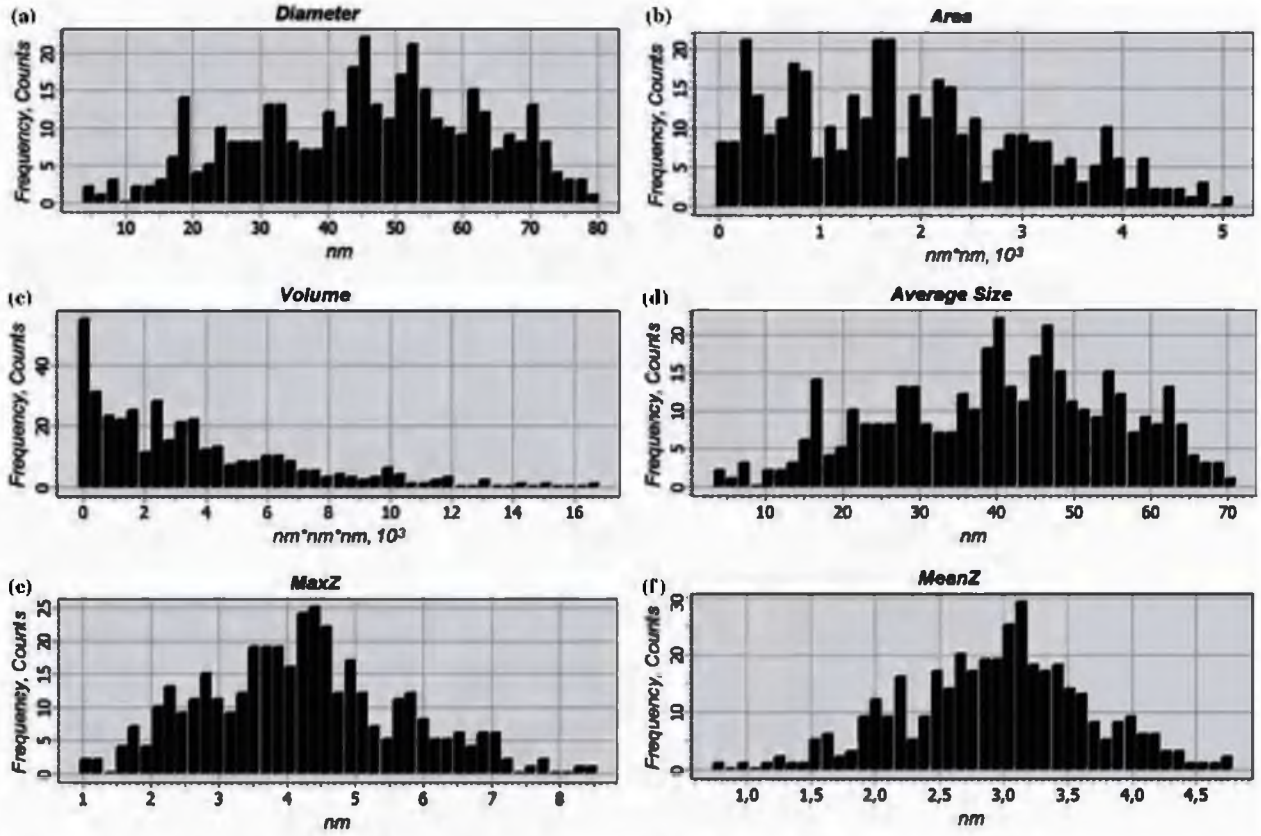

Fig. 6. Diagrams that shows the calculation of S- and 3D-parameters describing structure of the Si_3N_4 ($T_S = 40$ °C) film in the three-dimensional space.

show a dominant band at 982 cm $^{-1}$, in the spectral region characteristic for Si_3N_4.[13]

The layer surface morphology was studied by the contact mode atomic force microscopy (AFM) on Ntegra Aura (NT-MDT, Russia), using cantilevers CSG11 series in a controlled atmosphere or low vacuum. The Si_3N_4 film thickness was estimated by the step height at the edge of the film.

The interface between Si_3N_4 film and silicon substrate was investigated on cross section foils of the heterostructure Si_3N_4/Si(100) using the images and electron diffraction patterns obtained on a Jeol JEM 2100 transmission electron microscope.

3. RESULTS AND DISCUSSION

Investigation of the cross section of Si_3N_4/Si(100) heterostructure obtained at a substrate temperature $T_S = 40$ °C reveal a distinct boundary between the Si_3N_4 layer and Si(100) (Fig. 1). From the Figure 1(b) you can see a little ~1 nm texture that looks like parallel rows in the Si_3N_4 film directed perpendicularly to the Si substrate. Figure 2 shows the results of electron beam diffraction in a transmission electron microscope. Diffusion regions around the central diffuse reflex are typical for the amorphous material and the presence of ill-defined concentric rings indicating the presence of secondary nanocrystalline phase (Fig. 2(a)). Hence, the Si_3N_4 film is in a mixed amorphous and nanocrystalline state ($\alpha + \mu c$). Calculation of interplanar distances, which were made on the basis of electron diffraction, suggests that Si_3N_4 nanocrystals belongs to cubic system, space group Fd-3m. On the Figure 2(b) there is a clear picture of symmetrical reflexes spots corresponding to the single-crystal substrate Si(100).

Surface morphology of Si_3N_4 films obtained at substrate temperature $T_S = 40$, 300, 500 and 800 °C was studied using AFM (Fig. 3). Distribution function of profile height

Table I. Statistical analysis and processing of AFM-images for Si_3N_4 films obtained at a Si(100) substrate at the temperature $T_S = 40$ °C.

	Area	Average size	Length	Mean width	Aspect ratio	Volume	Range Z	Max Z	Min Z	Mean Z	Local mean Z	Perimeter	Diameter
Unit	nm * nm	nm	nm	Nm		nm * nm * nm	nm	nm	nm	nm	nm	nm	nm
Average	1925.081	41.276	58.026	29.674	2.135	3451.253	2.737	4.260	1.523	2.977	1.453	171.599	46.576
SD	1204.687	14.875	17.811	12.547	0.669	3152.873	1.415	1.418	0.362	0.702	0.664	64.205	16.785

Table II. Statistical treatment of AFM-images of Si_3N_4 film obtained at the Si(100) substrate with different temperatures $T_S = 40$ °C, 300 °C, 500 °C and 800 °C.

	T_S			
Parameters	40 °C	300 °C	500 °C	800 °C
S_z, Maximum peak height, nm	9.1	22.3	43.6	36.3
S_a, Average roughness, nm	1.1	2.2	4.9	3.9
S_q, Root mean square (RMS), nm	1.3	2.8	6.3	5.1
Average diameter, nm	46.5	39.3	60.6	38.8
S_{dr}, Surface area ratio, %	0.8	4.1	7.6	8.9

A(Z) was used for the mathematical description of the surface topography. This function gives the probability that a randomly selected point has a height Z. Figure 4 shows the evolution of the distribution function of altitude profile coating Si_3N_4 at substrate temperatures of 40, 300, 500 and 800 °C.

Statistical processing of the AFM images was performed using the software package "Image Analysis P9" (NT-MDT). The software package allows to calculate S-parameters (a surface area) or 3D-parameters,[14] characterizing the structure in three dimensions. Example and results of statistical processing of the obtained Si_3N_4 film at a substrate temperature $T_S = 40$ °C are presented in Figures 5 and 6 and Table I. A similar statistical analysis and processing of AFM-images was performed for Si_3N_4 films obtained at higher substrate temperatures.

From the AFM image analysis it was found that the increment of the surface area (S_{dr}) increased from 0.8% at $T_s = 40$ °C to 4.1, 7.6 and 8.9% at 300, 500 and 800 °C correspondingly (Table II). However, the average grain diameter 60 nm is maximal for the temperature of 500 °C. The minimum diameter of the grains is about 40 nm, which have the layers deposited at 300 and 800 °C. Coatings at a substrate temperature of 40 °C have the grain diameter of 45 nm. The maximum value of 6 nm of the mean-square roughness (S_q) was found for a substrate temperature of 500 °C. The minimum S_q value of 1 nm was obtained for the Si_3N_4 film deposited at 40 °C.

4. CONCLUSION

In this article, the dependence of the surface morphology of mixed ($\alpha + nc$) amorphous and nanocrystalline silicon nitride films Si_3N_4 depend on temperature were investigated by atomic force microscopy method. It was found that the growth substrate temperature up to $T_S =$ 800 °C increases the surface area of the film (mean-square roughness (S_q)) is more than 10 times. In the case of silicon nitride films as absorbing and antireflection layers in photovoltaic structures very large impact on the efficiency of solar energy conversion has both area and surface morphology of the outer layer. Structure of cross section ($\alpha + nc$) of the Si_3N_4/p-Si(100) heterostructure was investigated by transmission electron microscopy. It has been found that the Si_3N_4 film has a mixed character (amorphous and nanocrystalline phase). On the basis of electron diffraction studies it was found that the Si_3N_4 nanocrystals belonged to cubic system. It was found that a cross section of Si_3N_4 film was complex texture, composed of layers of about 1 nm, located perpendicular to the plane of the Si substrate and larger objects up to tens of nanometers, which is consistent with the results of AFM microscopy.

Acknowledgments: Research was accomplished with the support of Ministry of Education and Science of the Russian Federation, Reference number 367.

References and Notes

1. C.-H. Lee, K.-C. Park, and K. Kim. *Appl. Phys. Lett.* 87, 073510 (2005).
2. K. A. Nasyrov, S. S. Shajmeev, V. A. Gricenko, G. X. Han, S. V. Kim, and C. V. Li, *ZhETF* 129, 926 (2006).
3. D.-H. Neuhaus and A. Münzer, *Advances in Opto Electronics*, in special issue Volume, Article ID 24521, 15 pages (2007).
4. V. A. Gritsenko, *Physics - Uspekhi* 55, 498 (2012).
5. J. L. Cruz-Campa, et al., *Sol. Energy Mater. Sol. Cells* 95, 551 (2011).
6. A. Lennie, H. Abdullah, S. Shaari, and K. Sopian, *American Journal of Applied Sciences* 6, 2043 (2009).
7. V. Zakhvalinskii, E. Piliuk, I. Goncharov, A. V. Simashkevich, D. A. Sherban, L. I. Bruc, N. Curmei, and M. Rusu, *p-Si/n-SiC* nanolayer photovoltaic cell, *Proceedings of the 28th European Photovoltaic Solar Energy Conference*, Paris, France, September–October (2013).
8. J. Schmidt, J. D. Moschner, J. Henze, S. Dauwe, and R. Hezel, Recent progress in the surface passivation of silicon solar cells using silicon nitride, *19th European Photovoltaic Solar Energy Conference*, Paris, France, June (2004).
9. L. E. Hintzsche, C. M. Fang, T. Watts, M. Marsman, G. Jordan, M. W. P. E. Lamers, A. W. Weeber, and G. Kresse, *Physical Review B* 86, 235204 (2012).
10. Y. Tawada and H. Yamagishi, *Sol. Energy Mater Sol. Cells* 66, 95 (2001).
11. B. Rech, T. Roschek, J. Muller, S. Wieder, and H. Wagner, *Sol. Energy Mater. Sol. Cells* 66, 267 (2001).
12. Y. Hamakawa, *Journal de Physicque* 42(Suppl 10), C4-1131, (1981).
13. R. D. Mundo, R. d'Agostino, F. Fracassi, and F. Palumbo, *Plasma Process. Polym.* 2, 612 (2005).
14. L. Blunt and X. Jiang, Advanced Techniques for Assessment Surface Topography: Development of a Basis for 3D Surface Texture Standards "Surfstand," Kogan Page Science, London (2003).